INFLUENCE OF THE ARCHITECTURE OF FINE BUBBLE GENERATORS ON THE VARIATION OF THE CONCENTRATION OF OXYGEN DISSOLVED IN WATER

Nicolae BĂRAN[1], Ionela Mihaela CĂLUŞARU[2], Alexandru PĂTULEA[3]

The paper aims to present the influence of the constructive solution of fine bubble generators on the concentration of oxygen dissolved in water.

Original construction solutions for two types of fine bubble generators whose nozzles are manufactured by electro erosion are presented. The functioning conditions of fine bubble generators are presented and compared with the critical flow rate. The differential equation of the transfer speed of the oxygen towards water is numerically integrated, software is written and theoretical results are presented. A setup for experimental tests regarding the functioning of fine bubble generators was designed and built in the frame of the laboratory. Measurements regarding the increase of the concentration of oxygen dissolved in water were performed. Theoretical and experimental results were compared.

Keywords: fine bubble generators, water oxygenation

1. Introduction

The oxygenation, denoted also "aeration" in specialty literature, constitutes the main operation needed to assure an appropriate quality of water in water treatment and purification processes. The aeration is used [1][2]: in water treatment processes, in order to eliminate dissolved inorganic substances or chemical elements as iron, manganese etc. by oxidation and formation of sedimentable compounds or compounds that can be retained through boiling; for the biologic purification of wastewaters by the active mud process or in biofilters. The oxygenation equipment [2] is based on the dispersion of a phase in the other, for instance gas in liquid, energy-consuming process. The diffusion of oxygen in water is the most important factor to be considered in the conception and design stage of water oxygenation equipment.

The experimental researches have the following purpose:

Two constructive versions of fine bubble generators are compared:

- 1st version: the plate is of circular shape; air bubbles will configure a circular jet;

[1]Prof., Department of Thermotechnics, Engines, Thermic and Refrigeration Equipment, "Politehnica" University of Bucharest, Romania, e-mail: n_baran_fimm@yahoo.com
[2] PhD Student, Eng., "Politehnica" University of Bucharest, Romania
[3] PhD Student, Eng., "Politehnica" University of Bucharest, Romania

- 2nd version: the plate is of rectangular shape; air bubbles will configure a planar jet.

The researches intend to establish which version is the most efficient in respect to the variation of the concentration of oxygen dissolved in water in function of time; air pressure and flow rate of the compressed air introduced in water remain constant in both versions.

2. Constructive solutions of fine bubble generators

Two constructive versions were designed in function of the shape of the nozzle plate fixed on the body of the fine bubble generator (FBG):

- 1st version: the plate is of circular shape; it is fixed on a cylindrical body of the fine bubble generator, leading to the name of "circular shape FBG";
- 2nd version: the plate is of rectangular shape; it is fixed on the FBG body, in this case a nozzle with rectangular output section; hereupon the FBG is called "rectangular shape FBG".

In both versions the nozzle plate material is alumina of thickness s = 2 mm. The nozzles were manufactured by electro erosion using a Φ0.5 mm electrode. Conditions found in specialty literature [3][4] were observed when building fine bubble generators:

$$\frac{s}{d_0} > 3\,; \frac{d}{d_0} > 8\,. \tag{1}$$

where: d_0 – nozzle diameter, $d_0 = 2r_0$; d – distance between axes of two consecutive nozzles; D_0 – diameter of gas bubble at nozzle output (in the moment of its detachment); s – plate thickness.

Interaction among bubbles during formation can be neglected if a distance greater than eight diameters among the rigid nozzles of the plates is provided [4].

Conditions (1) become:

$$\frac{s}{d_0} = \frac{2}{0.5} = 4 > 3; \frac{d}{d_0} = 10 > 8$$

The diameter of a gas bubble at the nozzle output is $D_0 \approx 2d_0$; $D_0 = 2R_0$; hereupon, in order to obtain fine bubbles ($D_0 < 1$ mm), the nozzle diameter has to be as small as possible, $d_0 < 0.5$ mm. Both constructive versions feature the same network step: $d = 10 \cdot d_0 = 10 \cdot 0.5 = 5$ mm and an equal number of nozzles: n = 37.

A value of $d = 10 \cdot d_0$ was chosen for the second condition; it is also verified that the radius of the gas bubble arrived to the free surface of the water (R_b) satisfies the condition $R_b < d$, thus the gas bubble coalescence is avoided.

In the case of dynamic conditions, the frequency of gas bubble forming tends to be constant; the initial radius of the bubble is computed using [5]:

$$R_0 = \frac{1}{2}\left(\frac{81\cdot\eta\cdot\dot{V}}{\pi\cdot\rho\cdot g}\right)^{\frac{1}{4}} = \frac{1}{2}\left(2.629\cdot\nu\cdot\dot{V}\right)^{\frac{1}{4}} = 1.475\cdot10^{-3}\ \ [m] \tag{2}$$

It can be noticed that R_0 does not depend on r_0, but on $\dot{V}$ and ν. The relation is stable for high viscosity liquids, for instance glycerine. The bubble radius is given by [5]:

$$R_b = R_0\left(1+\frac{\rho g H}{p_{atm}}\right)^{\frac{1}{3}} \tag{3}$$

It is considered that H=1.5 m and $\rho_{H2O}=10^3$ kg/m^3; relation (3) leads to:

$$R_b = 1.475\cdot10^{-3}\left(1+\frac{10^3\cdot9.81\cdot1.5}{101325}\right)^{\frac{1}{3}} = 1.689[mm] \tag{4}$$

- 1st version

The 37 Φ 0.5 mm nozzles were disposed as to create a "circular" bubble column; nozzle repartition on the circular plate can be noticed from figure 1, all of them being included in a Φ35 mm circle.

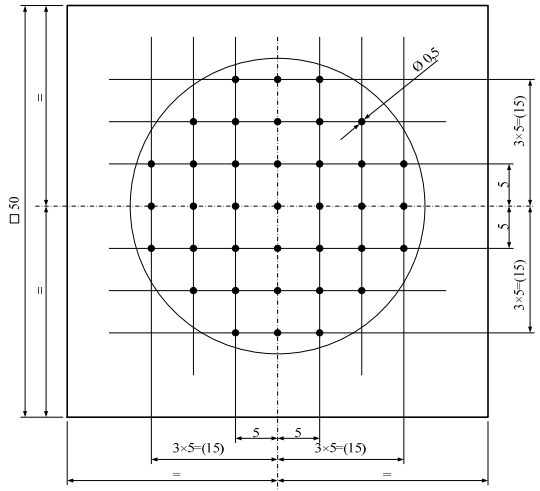

Fig. 1. Sketch of the first version of perforated plate.

The plate of Fig. 1 constitutes the main element of the circular shape FBG presented in figures 2.a (view) and 2.b (section view).

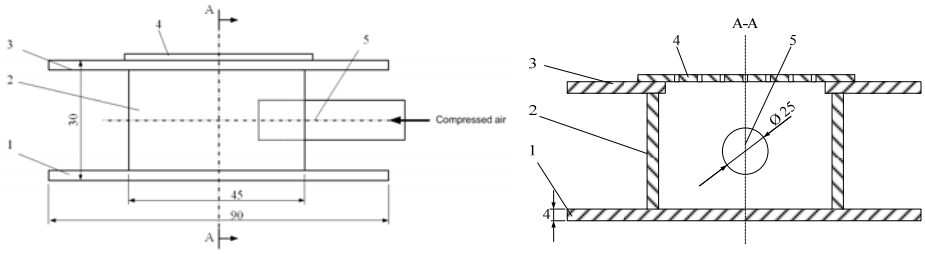

a) b)

Fig. 2. Circular shape FBG.

a) view: 1- base plate; 2 – Φ35 cylinder; 3 – upper plate; 4 – nozzle plate; 5 – air feed pipe. b) section view: 1- base plate; 2 –Φ35 cylinder; 3 – upper plate; 4 – nozzle plate; 5 – compressed air feed pipe

- 2nd version

The 37 Φ 0.5 mm nozzles were disposed on a sole row, so that the bubble columns create a bubble curtain similar to the one formed by a planar jet with a rectangular shape transversal section. The repartition of the Φ 0.5mm nozzles can be noticed in figure 3.

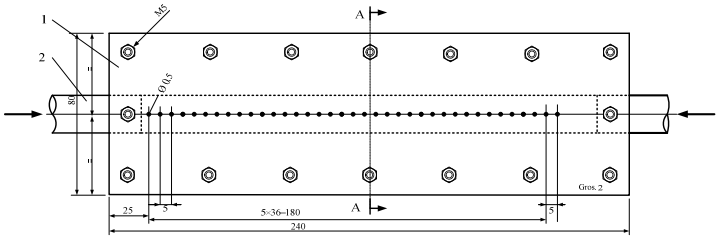

Fig. 3. Sketch of the second version of perforated plate
1- nozzle plate; 2- compressed air feed pipe.

A rotated view of the section A-A from Fig. 3 is presented in Fig. 4.

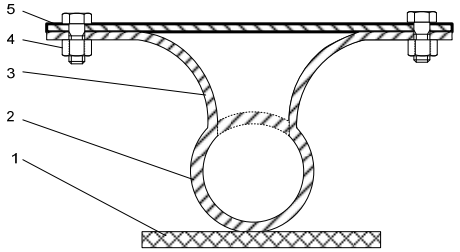

Fig. 4. Section from the rectangular shape FBG.
1 – holder; 2 – compressed air feed pipe; 3 – FBG body; 4 – screws for fastening the plate on the body; 5 – nozzle plate.

The plate from figure 3 is fastened with screws on the body of the FBG (figure 4), the result being the assembly of figure 5.

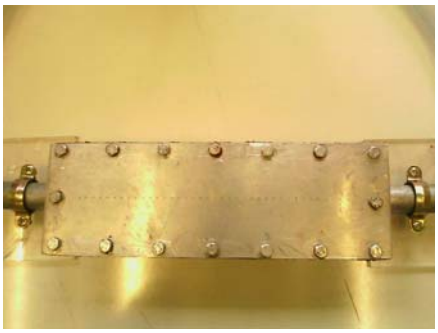

Fig. 5. The FBG assembly: FBG body and the plate fastened with screws.

A special sealing system, proof to water action, is provided between the nozzle plate and the flange of the FBG body.

3. Establishing the FBG functioning conditions

In function of the gas flow rate ($\dot{V}$), the bubble generating conditions can be classified in three categories [7]: quasi-static conditions ($\dot{V} < \dot{V}_{cr}$); dynamic conditions ($\dot{V} \geq \dot{V}_{cr}$); turbulent conditions ($\dot{V} >> \dot{V}_{cr}$). The quasi-static and dynamic conditions are separated by the value of the critical flow rate. The critical flow rate for water/air as working fluids and 0.1…2 mm nozzles can be computed using [3][5]:

$$\dot{V}_{cr} = \pi \left(\frac{16}{3g^2} \right)^{\frac{1}{6}} \left(\frac{\sigma \cdot r_0}{\rho_{H2O}} \right)^{\frac{5}{6}} \tag{5}$$

where : g – gravitational acceleration, g=9.81 m/s^2; σ- surface tension coefficient; for water $\sigma = 8 \cdot 10^{-2}$ N/m; $\rho_{H_2O} = 10^3$ kg/m^3, r_0–nozzle radius [m].

The values of σ, r_0, ρ_{H_2O} are the same for both versions, thus $\dot{V}_{cr}$ will be the same. It is obtained that:

$$\dot{V}_{cr} = 3.14 \left(\frac{16}{3 \cdot 9.81^2} \right)^{\frac{1}{6}} \left(\frac{8 \cdot 10^{-2}}{10^3} \right)^{\frac{5}{6}} \cdot r_0^{\frac{5}{6}} = 0.745 \cdot 10^{-3} r_0^{\frac{5}{6}} \quad [\text{m}^3/\text{s}] \tag{6}$$

For $r_0 = 0.25 \cdot 10^{-3}$ [m] it is obtained that :

$$\dot{V}_{cr} = 0.745 \cdot 10^{-3} \left(0.25 \cdot 10^{-3} \right)^{\frac{5}{6}} = 0.744 \cdot 10^{-6} \ [\text{m}^3/\text{s}] = 2.678 \ [\text{dm}^3/\text{h}] \tag{7}$$

Due to the fact that the perforated plate contains 37 nozzles, the gas flow rate for the whole plate will be:

$$\dot{V}_{cr} = 37 \cdot 2.678 = 99.08 \ [\text{dm}^3/\text{h}] \tag{8}$$

The next step of the computation is to find the air flow speed through the nozzles and the minimum flow rate for which the first air bubbles appear.

It is known from specialty literature [5][6] that, in the case of gas flow in conditions of small pressure drops, if the initial speed of the gas jet and the geometrical pressure are neglected, the speed of gas at the nozzle output can be computed using:

$$w = \sqrt{\frac{2\Delta p}{\rho}} \quad \left[m/s \right] \tag{9}$$

where: Δp – static pressure drop; ρ – gas density.

The static pressure drop can be assimilated to the pressure drop on a local resistance (nozzle flow), magnitude that has been measured and is equal to 20.4 mmH_2O. This value is close to the one existing in specialty literature [7].

Air density is computed from the thermic state equation:

$$\rho = \frac{p}{RT} \quad \left[kg/m^3 \right]; p = p_{atm} + p_H + p_{ts} + \Delta p \tag{10}$$

where: p_{atm} – atmospheric pressure, 101325 N/m^2, p_H – hydrostatic load, 500 mmH_2O, p_{ts} – pressure due to surface tension, 63 mmH_2O, Δp – pressure drop on nozzle, 20 mmH_2O; R- air constant.

$$p_H + p_{ts} + \Delta p = 500 + 63 + 20 = 583 \quad mmH_2O$$

$$p = p_{atm} + \rho_{H_2O} g \left(p_H + p_{ts} + \Delta p \right) \quad \left[N/m^2 \right] \tag{11}$$

$$\rho = \frac{101325 + 9.81 \cdot 583}{287 \cdot \left(24 + 273.15 \right)} = 1.26 \quad \left[kg/m^3 \right] \tag{12}$$

$$w = \sqrt{\frac{2 \cdot 9.81 \cdot 20.4}{1.26}} = 17.64 \quad \left[m/s \right] \tag{13}$$

The blasting air output section area is equal to:

$$A = n \cdot \frac{\pi d^2}{4} = 37\pi \frac{\left(0.0005 \right)^2}{4} = 7.27 \cdot 10^{-6} \quad \left[m^2 \right] \tag{14}$$

The flow rate of the blasting air will be:

$$\begin{aligned} \dot{V} &= Aw = 7.27 \cdot 10^{-6} \cdot 17.64 = 0.12825 \cdot 10^{-3} \quad \left[m^3/s \right] \\ \dot{V} &= 0.12825 \cdot 10^{-3} \cdot 10^3 \cdot 3600 = 462.6 \quad \left[dm^3/h \right] \end{aligned} \tag{15}$$

First air bubbles emitted by the FBG begin to appear at this flow rate. For a continuous and safe functioning, it was decided that the air flow rate would equal 600 dm^3/h. Accordingly the experimental researches will be performed with

the following values of the blasting air: $\dot{V}_1 = 600 \ \ dm^3/h$ and p_1=583 mmH_2O; the hydrostatic load is equal to H = 500 mmH_2O. Because: $\dot{V}_1 = 600\left[dm^3/h\right]$ and $\dot{V}_{cr} = 99.8\left[dm^3/h\right]$, [8][9], it results that the FBG will function in dynamic conditions.

4. Theoretic establishment of the variation of the concentration of oxygen dissolved in water in function of the oxygenation process duration

The equation of the transfer speed of oxygen towards water has the following shape [10][11][12]:

$$\frac{dC}{d\tau} = ak_L(C_s - C) \ \left[\frac{kg}{m^3 s}\right] \tag{16}$$

where: $\frac{dC}{d\tau}$ – transfer speed of dissolved oxygen [$kg/m^3 \cdot s^{-1}$]; ak_L–volumetric mass transfer coefficient [*1/s*]; C_s – mass concentration of the transferable component at saturation (at equilibrium) in the liquid phase [kg/m^3]; C – current mass concentration of the transferable component in the liquid phase [kg/m^3].

In order to theoretically establish the variation of the concentration of oxygen dissolved in water in function of the water oxygenation process duration for the 1st version of FBG the following magnitudes have to be known: initial concentration of the oxygen dissolved in water for the temperature t=20.5 ^oC; C_1=7.72 mg/l; saturation concentration for the same temperature and p=750mmHg is equal to C_s=8.9 mg/l; duration of the oxygenation process τ=120 min; integration step h=1 min; n=120/1=120 values are needed in order to build the chart $C = f(\tau)$; the value aK_L is established using the integral method [5] for the first two time intervals: 0 →15'; 15'→30' using (17):

$$aK_L = \frac{1}{\tau_2 - \tau_1} ln \frac{C_s - C_1}{C_s - C_2} [\text{min}^{-1}] \tag{17}$$

where C_1 and C_2 denote the concentration of O_2 in water at the time moments τ_1 and τ_2. If (17) is applied in the case of rectangular shape FBG, it results that:

$$\text{I)} \ \tau_1=0' \rightarrow \tau_2=15' \rightarrow aK_{Ld} = \frac{1}{15-0} ln \frac{8.9-7.72}{8.9-8.30} = 0.0363 \ [\text{min}^{-1}] \tag{18}$$

$$\text{II)} \ \tau_1=15' \rightarrow \tau_2=30' \rightarrow aK_{Ld} = \frac{1}{30-15} ln \frac{8.9-8.30}{8.9-8.53} = 0.0490 \ [\text{min}^{-1}] \tag{19}$$

Thus computations lead to a mean value of 0.0427 [min^{-1}] for the coefficient aK_{Ld}. This value is needed as input for the computation software written in order to build the chart $C = f(\tau)$. Similar computations are performed for circular shape FBGs, leading to a mean value of 0.0591[min^{-1}] for the coefficient

aK_{Lc}. 120 points of the function $C=f(\tau)$ were obtained from the computation software. Their graphical representation leads to the chart presented in figure 6.

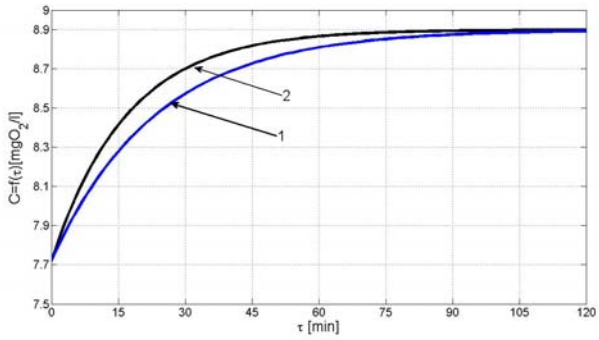

Fig. 6. The variation $C=f(\tau)$ established by numerical integration of the differential equation regarding the transfer speed of O_2 in water; 1 – chart based on theoretical results in the case of rectangular shape FBG; 2 – chart based on theoretical results in the case of circular shape FBG

It can be noticed from figure 6 that the current concentration of O_2 in water reaches C_s after about 120 minutes. These theoretical results will be compared to those experimentally established.

5. The FBG test setup

The laboratory plant where measurements are performed is presented in figure 7. Compressed air pressure and air flow rate were kept constant during measurements.

6. Measurement method and experimental results

The two constructive versions of FBG will be tested separately. Measurements regarding O_2 concentration will be performed separately as well.

6.1. Working hypotheses

Two versions (1^{st} and 2^{nd}) of FBG were conceived and built in order to establish the influence of FBG architecture on O_2 concentration in water.

The following working hypotheses were observed during FBG building and experimental tests: same area of the output section of air in water for both versions; same flow rate of the air blasted in water; same temperature, air pressure and water pressure during the tests of both FBG; same hydrostatic load; same initial concentration of oxygen dissolved in water; same duration of the oxygenation process and same measurement method.

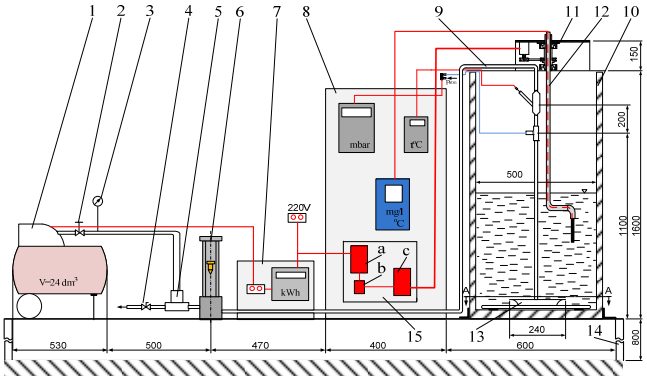

Fig. 7. Sketch of the experimental setup for researches regarding water oxygenation
1– electro compressor with air tank; 2 - pressure reducer;3–manometer; 4–joint for exhausting of air in the atmosphere; 5– compressor feeder; 6– rotameter; 7– electric panel; 8– measuring instruments panel; 9– pipe for the transport of the compressed air towards the FBG; 10– water tank; 11– mechanism for probe driving; 12– oxygen meter probe; 13– FBG; 14– holder for the plant; 15–control electronics (a – supply unit, b- switch, c- control element).

6.2. The measurement process

For the first version of FBG, the measurements were performed in eight stages. At the beginning of the first stage, the situation is described by figure 7, where the height of the water layer over the FBG is h_{H2O} = 500 mm, the probe is situated at h_{probe} = 250 mm with respect to the nozzle plate, the initial O_2 concentration being C_0 =7.72 mg/l, the indication of the electric counter E_0 = 0.0325 kWh and water temperature t= 20.5°C. Pressure and flow rate of air that enters the FBG are measured: p_1=583.44 mmH_2O; $\dot{V}_1$= 600 l/h. After a functioning of the FBG for $\Delta\tau_1$ =15', it is stopped and O_2 concentration is measured by rotating the probe in water. The FBG is put in functioning again and air is blasted in water during 15', the total time being $\Delta\tau_2$ =30'; O_2 concentration is measured. Similarly, the time values of $\Delta\tau_3$ =45', $\Delta\tau_4$ =60', $\Delta\tau_5$ =75', $\Delta\tau_6$ =90', $\Delta\tau_7$ =105', $\Delta\tau_8$ =120' are reached. Finally, the concentration of O_2 dissolved in water after two hours of FBG functioning is measured.

The measured values are presented in table 1.

Table 1

Variation of O_2 concentration [mg/l] in function of the functioning time of the FBG

τ=0′	$\Delta\tau_1$=15′	$\Delta\tau_2$=30′	$\Delta\tau_3$=45′	$\Delta\tau_4$=60′	$\Delta\tau_5$=75′	$\Delta\tau_6$=90′	$\Delta\tau_7$=105′	$\Delta\tau_8$=120′
7.72	8.02	8.34	8.43	8.54	8.54	8.57	8.59	8.59

The chart C_{O2}= f(τ), curve no.2 from figure 8, is traced based on data presented in table 1.

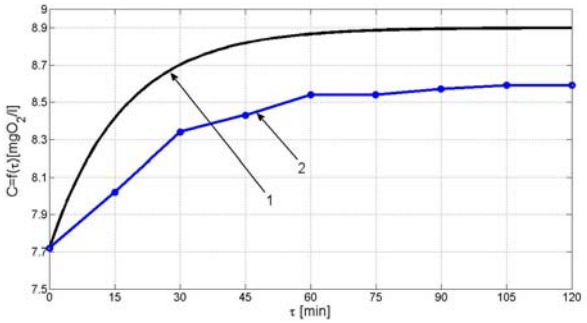

Fig. 8. Variation of the concentration of O_2 in water in function of time (for the 1st version); 1-chart based on theoretical results; 2- chart based on experimental data.

The first point of the chart represents the concentration of O_2 dissolved in water at the beginning of the measurements ($\tau=0'$); after each stage of FBG functioning the concentration of dissolved oxygen (O_2) will be marked by points (•) in figure 8. Neither the metabolism of microorganisms (see reactors, water treatment plants) neither fishes consumed the oxygen transferred in clean water (supply network water), hereupon the concentration of oxygen in water increased according as air was blasted in the water tank. Figure 8 proves good coincidence between the theoretical calculation model and obtained experimental results.

Similar procedures are applied for the 2nd version of FBG. The tank is emptied, is refilled with fresh water and measurements are performed such as for the 1st version. The results are presented in table 2.

Table 2

Variation of the O_2 concentration [mg/l] in function of the functioning time of the FBG

$\tau=0'$	$\Delta\tau_1=15'$	$\Delta\tau_2=30'$	$\Delta\tau_3=45'$	$\Delta\tau_4=60'$	$\Delta\tau_5=75'$	$\Delta\tau_6=90'$	$\Delta\tau_7=105'$	$\Delta\tau_8=120'$
7.72	8.30	8.53	8.72	8.78	8.84	8.85	8.85	8.85

The chart $C_{O2}= f(\tau)$, curve no.2 from figure 9, is traced based on data presented in table 2. Good coincidence of the two curves is noticed.

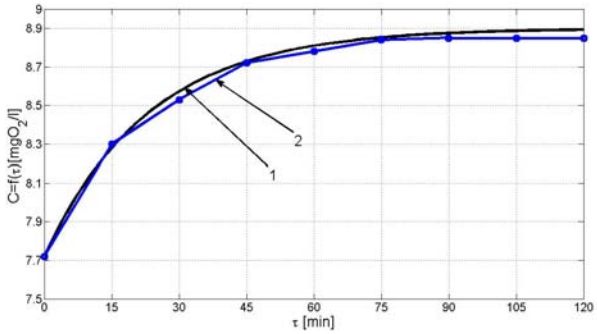

Fig. 9. Variation of the concentration of O_2 in water in function of time (for the 2nd version); 1-chart based on theoretical results; 2- chart based on experimental data.

6.3. Final results of the experimental researches

Curves presented in figure 10 were traced on the basis of theoretical and experimental data.

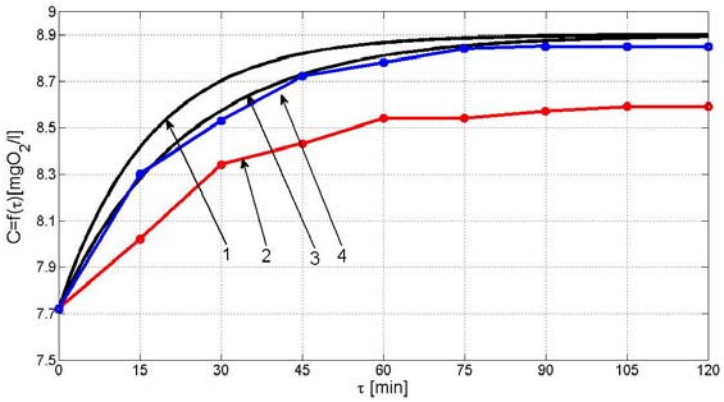

Fig. 10. Variation of the concentration of oxygen dissolved in water in function of time
1 - curve based on theoretical results obtained in the case of circular shape FBG; 2 - curve based on experimental results obtained for the 1st version of FBG (circular shape FBG); 3 - curve based on theoretical results obtained in the case of rectangular shape FBG; 4 - curve based on experimental results obtained for the 2nd version of FBG (rectangular shape FBG).

It can be noticed from figure 10 that the 2nd version is more beneficial; the obtained results are compared to data existing in specialty literature [5][13][14][15].

7. Conclusions

Two types of FBG were theoretically and experimentally analyzed: one of circular shape and one of rectangular shape. The analysis marked out the following aspects:

1) The increase of O_2 concentration in water in function of the oxygenation process duration is more beneficial in the case of rectangular shape FBG.

2) Rectangular shape FBG offers a more outspread way of placing the air immersion nozzles and a better contact of the air bubble with the water mass.

3) The solution that uses circular shape porous spreaders is not recommended for use, because it does not assure a uniform repartition of air bubbles and, moreover, leads to high pressure losses.

4) Performed experimental researches prove that the rectangular shape FBG are more advantageous. The mounting of 3-5 rows of rectangular shape

FBGs leads to a fine bubble curtain that can oxygenate a layer of running water; this situation can happen in water treatment plants and in fish breeding tanks.

R E F E R E N C E S

[1] *D. Robescu, D.L. Robescu,* Methods, plants and equipment for the physical purification of wastewater (in Romanian), Bren Publishing House, Bucharest, 1999.

[2] *D. Robescu, D.L. Robescu, S. Lanyi, A. Verestoy,* Reliability of processes and plants for water treatment and purification (in Romanian), Technical Publishing House, Bucharest, 2002.

[3] *G. Oprina*, Contributions of the hydro-gas-dynamics of porous diffusers (in Romanian), PhD Thesis, POLITEHNICA University of Bucharest, Faculty of Power Engineering, 2007.

[4] *T. Miyahara, Y. Matsuha, T. Takahashi,* The size of bubbles generated from perforated plates*,* International Chemical Engineering 23, 1983, pp. 517-523.

[5] *G. Mateescu*, Hydro-gas-dynamics of fine bubble generators (in Romanian), PhD Thesis,, POLITEHNICA University of Bucharest, Faculty of Mechanical Engineering and Mechatronics, Bucharest, 2011.

[6] *Al. Dobrovicescu, N. Băran*, ş.a., Elements of Technical Thermodynamics (in Romanian), POLITEHNICA PRESS Publishing House, Bucharest, 2009.

[7] *G. Oprina, Gh. Băran, ş.a.,* Establishment of global aerodynamic resistance factors in the case of perfored plates (in Romanian), Proceedings of the 6th Conference of Romanian Hydro Power Engineers «DORIN PAVEL« 27-28 May 2010, Bucharest, pp. 51 – 60.

[8] *G. Oprina, I. Pincovschi, Gh. Băran*, Hydro-gas-dynamics of aeration systems equipped with fine bubble generators (in Romanian), POLITEHNICA PRESS Publishing House, Bucharest, 2009.

[9] *N. Băran, Gh. Băran, G. Mateescu*, Research Regarding a New Type of Fine Bubble Generator, Romanian Review of Chemistry, **vol. 61**, no.2, 2010, pp. 196-199, ISSN 0034-7752.

[10] *N. Băran, Al. Pătulea, Gh. Băran*, Experimental researches regarding the obtaining of curtains of fine air bubbles, Proceedings of the 6th Conference of Romanian Hydro Power Engineers «DORIN PAVEL« 27-28 May 2010, Bucharest, pp. 23 – 32.

[11] *I. Pincovschi*, Hydrodynamics of disperse gas-liquid systems (in Romanian), PhD Thesis, POLITEHNICA University of Bucharest, Faculty of Power Engineering, 1999.

[12] *N. Băran, Gh. Băran, G. Mateescu, Al. Pătulea*, Water oxigenation, Bulletin of the Polytechnic Institute of Jassy, tome LVI (LX) fasc.3b, POLITEHNIUM Publishing House 2010, pag.78-83.

[13] *N. Băran, A. Zaid, Al. Pătulea*, Researches regarding the increase of the dissolved oxygen concentration in function of the duration of the water oxygenation process, TERMOTEHNICA, No .2/2010, pp. 15-18, ISSN 1222-4057.

[14] *V.V.Buwa, V.V.Ranade*, Dinamisc of gas-liquid flow in a recrangular bubble column; experiments and single/multi group DFD simulation, CHEMICAL ENGINEERING SCIENCE, No.57, 2002,pp4715-4736 .

[15] E.Becerril, A.Corkx, Effect of bubble deformation on stability and mixing in bubble colums, CHEMICAL ENGINEERING SCIENCE, No.57, 2002,pp.3283-3297.